PERGAMON

Chemical Engineering Science 58 (2003) 3659–3668

Chemical Engineering Science

www.elsevier.com/locate/ces

Characteristics and reactivities of $Ca(OH)_2$/silica fume sorbents for low-temperature flue gas desulfurization

Ren-Bin Lin, Shin-Min Shih*, Chiung-Fang Liu

Department of Chemical Engineering, National Taiwan University, Taipei 106, Taiwan

Received 8 November 2002; received in revised form 21 April 2003; accepted 29 April 2003

Abstract

$Ca(OH)_2$/silica fume sorbents were prepared with various $Ca(OH)_2$/silica fume weight ratios and slurrying times at 65°C and a water/solid ratio of 10/1. Dry sorbents prepared were characterized, and their reactivities toward SO_2 were measured in a differential fixed-bed reactor at the conditions similar to those in the bag filters in the dry and semidry flue gas desulfurization (FGD) processes. The reaction between $Ca(OH)_2$ and silica fume in the slurry was very fast. The formation of calcium silicate hydrates, which were mainly C–S–H(I), resulted in sorbent particles with a highly porous structure that seemed compressible under high pressures. The sorbents were mesoporous, and their specific surface areas and pore volumes were much larger than those of $Ca(OH)_2$ alone. The utilization of Ca of sorbent increased with increasing silica fume content mainly due to the increase in the specific surface area of sorbent. The sorbent with 70 wt% $Ca(OH)_2$ had the maximum 1 h SO_2 capture. Sorbents with $Ca(OH)_2$ contents less than 100 wt% and greater than 21 wt% would have a SO_2 capture greater than that of $Ca(OH)_2$ alone. Both the 1 h utilization of Ca and SO_2 capture per unit specific surface area of sorbent decreased in general with increasing specific surface area. At the same $Ca(OH)_2$ content, the 1 h utilization of Ca or SO_2 capture of the $Ca(OH)_2$/silica fume sorbent was greater than that of the $Ca(OH)_2$/fly ash sorbent; however, the amount of SO_2 captured per unit surface area of the former sorbent was smaller than that of the latter sorbent. The results of this study are useful to the preparation of silica-enhanced sorbents for use in the dry and semidry FGD processes.

Keywords: Flue gas desulfurization; $Ca(OH)_2$; Silica fume; Structural properties; Reaction kinetics; Pollution control

1. Introduction

Combustion of fossil fuels, such as coal and oil, results in SO_2 formation. Reduction of SO_2 emissions is a major issue of environmental protection. Many flue gas desulfurization (FGD) processes are available for the reduction of SO_2 emissions (Miller, 1986; Srivastava & Jozewicz, 2001). Among these processes, the semidry and dry FGD processes have the advantages of requiring smaller space, being easier to retrofit, and producing dry solid product. However, the sorbent, which is typically hydrated lime, is not highly converted in the operation of these processes. How to increase the sorbent reactivity and utilization has been an important subject for the application of these processes.

Many researchers have shown that hydrated lime can be activated by reacting with siliceous materials, such as fly ash (Jozewicz & Rochelle, 1986; Peterson & Rochelle, 1988, 1990; Peterson, 1990; Martinez, Izquierdo, Cunill, Tejero, & Querol, 1991; Diffenbach, Hilterman, Frommell, Boother, & Hedges, 1991; Ho & Shih, 1992, 1993; Kind, Wasserman, & Rochelle, 1994; Kind & Rochelle, 1994; Sanders, Keener, & Wang, 1995; Tsuchiai, Ishizuka, Ueno, Hattori, & Kita, 1995; Al-Shawabkeh, Matsuda, & Hasatani, 1995; Garea et al., 1997a; Fernández, Renedo, Garea, Viguri, & Irabien, 1997; Renedo, Fernández, Garea, Ayerbe, & Irabien, 1999; Ishizuka, Tsuchiai, Murayama, Tanaka, & Hattori, 2000; Liu, Shih, & Lin, 2002), diatomaceous earth (Jozewicz, Chang, Sedman, & Brna, 1988a; Jozewicz, Jorgensen, Chang, Sedman, & Brna, 1988b), and silica (Chiu, 1989; Chiang, 1994; Kind, 1994; Jung, Kim & Kim, 2000a, b), in the presence of water, and the sorbents thus obtained have higher capacity of SO_2 capture and degree of Ca utilization than hydrated lime has. During the activation process, the active silica contained in siliceous materials reacts with hydrated lime to form calcium silicate hydrates ($xCaO \cdot SiO_2 \cdot yH_2O$); this reaction is called

* Corresponding author. Tel.: +886-2-23633974; fax: +886-2-23623040.
E-mail address: smshih@ccms.ntu.edu.tw (S.-M. Shih).

0009-2509/03/$ - see front matter © 2003 Elsevier Ltd. All rights reserved.
doi:10.1016/S0009-2509(03)00222-7

"pozzolanic reaction" (Taylor, 1964). It is believed that the pozzolanic reaction is responsible for the enhancement of the sorbent reactivity (Jozewicz & Rochelle, 1986; Peterson & Rochelle, 1988; Ho & Shih, 1992, 1993; Sanders et al., 1995; Lin, Shih, & Liu, 2002).

Among the siliceous materials, fly ash has attracted the most attention because it is the solid waste produced in coal-fired power plants. Only some research work on the sorbents prepared with pure silicas, such as quartz (Jung et al., 2000a, b) and silica fume (Chiu, 1989; Chiang, 1994; Kind, 1994; Lin, 1998; Liu, 1999), has been done. Fly ash contains both quartz and amorphous silica. The amorphous silica is more active than the crystalline quartz, therefore it predominates in participating in the pozzolanic reaction. Because silica fume is an amorphous silica, its reaction with $Ca(OH)_2$ can closely simulate the pozzolanic reaction between fly ash and $Ca(OH)_2$, thus the study on sorbents prepared with silica fume will enhance the understanding of the reactivities of $Ca(OH)_2$/fly ash sorbents. On the other hand, silica fume is an industrial waste that forms during the productions of silicon and silicon-containing alloys (Grutzeck, Atkmson, & Roy, 1983). A successful use of this alternative silica source for the activation of $Ca(OH)_2$ also has the merit of waste utilization.

In this work, $Ca(OH)_2$/silica fume sorbents were prepared with various $Ca(OH)_2$/silica fume weight ratios and slurrying times. Sorbents were characterized and their reactivities toward SO_2 were measured. The relations between the reactivity and properties of sorbent were analyzed.

2. Experimental section

2.1. Preparation of sorbents

Reagent grade $Ca(OH)_2$ (purity > 95%; Hayashi Pure Chemical Industries, Ltd.) and commercial silica fume (Finesil X70, purity > 94%; Tokuyama Soda Co., Ltd.) were used to prepare the sorbents. The physical properties of these starting materials are shown in Table 1.

The $Ca(OH)_2$ and silica fume, together with 80 g of deionized water, were placed into a 250 ml polypropylene flask at a water/solid weight ratio (L/S) of 10. The $Ca(OH)_2$/silica fume weight ratios tested were 0/10, 1/9, 3/7, 5/5, 7/3, 9/1, and 10/0. The flask was sealed with a rubber stopper at the mouth and inserted into a water bath at 65°C. The slurry was stirred with a magnetic stirrer. The samples with a ratio of 7/3 were stirred for different periods from 25 min to 16 h; the samples with other ratios were stirred for 16 h. After slurrying, the slurry was placed in a vacuum oven to evaporate the water; the solid phase left was further vacuum-dried at 110°C. The dried cake obtained was crashed into powder and sealed in a bottle before subjecting to characterization and sulfation test.

Table 1
Physical properties of $Ca(OH)_2$ and silica fume

Physical properties	$Ca(OH)_2$	Silica fume
Particle mean diameter (μm)	7.4	6.3
BET specific surface area (m^2/g)	9.6	220
True density (g/cm^3)	2.29	2.93
Porosity	0.45[a]	0.84[b]

[a]Pore dia. ⩽ 1 μm, measured by mercury intrusion method.
[b]Pore dia. ⩽ 0.3 μm, measured by N_2 adsorption.

2.2. Sulfation test

Experiments for the reaction of sorbents with SO_2 were carried out using a differential fixed-bed reactor under the conditions of 60°C, 70% RH, and 1000 ppm SO_2 up to 1 h. The experimental conditions were the typical bag filter conditions in dry and semidry FGD processes. About 20 mg of sample was used for each run. The total gas flow rate was 4 l/min (STP). CO_2 and O_2 were not added into the gas mixture because their presence produced little effect on the SO_2 uptake of sorbent at this low temperature (Garea, Viguri, & Irabien, 1997b). The experimental setup and procedure were described in detail in previous work (Ho & Shih, 1992; Liu, 1999). At least two replicate measurements were made for each sorbent.

The reactivity of sorbent toward SO_2 was expressed as the utilization of Ca and the SO_2 capture. The utilization of Ca or the conversion of $Ca(OH)_2$ for a reacted sample was determined by its SO_3^{2-}/Ca^{2+} molar ratio. The SO_3^{2-} content in a sample was determined by iodometric titration, and the Ca^{2+} content by EDTA titration. The SO_2 capture (SC) for a sample was defined as the ratio of the weight of the SO_2 captured to the initial weight of the sample. SC is related with the utilization of Ca by

$$\mathrm{SC} = M_{\mathrm{SO}_2} M^{-1}\ \text{Utilization of Ca}, \quad (1)$$

where M_{SO_2} is the molecular weight of SO_2, M is the initial sorbent weight per mole of Ca. M was calculated from the $Ca(OH)_2$/silica fume weight ratio for the sample.

2.3. Chemical and physical analyses

The sorbents were subjected to X-ray diffraction (XRD) analysis using a Mac Science M03XHF X-ray diffractometer. Scanning electron microscope (SEM), Hitachi S-2400, was used to observe the sorbent morphology. The sorbent particle size distribution was measured by laser diffraction using a Coulter LS-230 analyzer. The specific surface area of sorbent was determined from the nitrogen adsorption data by the BET method and the pore volume distribution was determined from the nitrogen desorption isotherm by the BJH method, using a Micromeritics ASAP 2010 analyzer. Prior to the measurement of N_2 adsorption, the sample was degassed under vacuum at a temperature of 65°C for 8 h in order to deplete the adsorbed gas molecules. Further experimental details were described elsewhere (Lin, 1998).

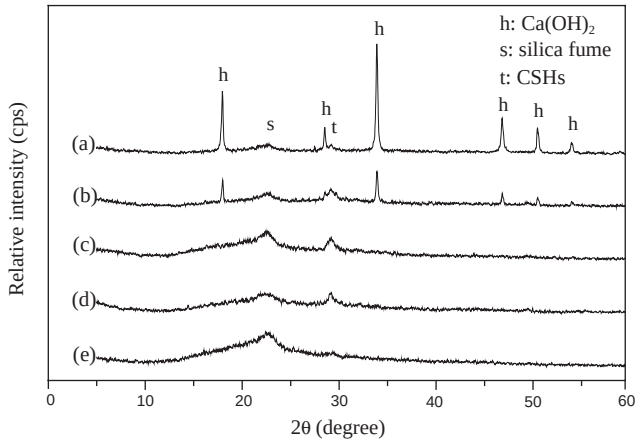

Fig. 1. XRD patterns of $Ca(OH)_2$/silica fume sorbents prepared with various $Ca(OH)_2$/silica fume weight ratios: (a) 9/1, (b) 7/3, (c) 5/5, (d) 3/7, (e) 1/9; slurrying conditions: 65°C, $L/S = 10/1$, and 16 h.

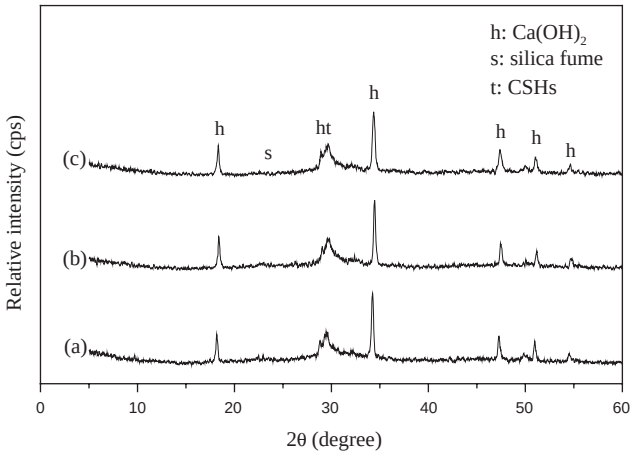

Fig. 2. XRD patterns of $Ca(OH)_2$/silica fume (wt. ratio 7/3) sorbents prepared with various slurrying times: (a) 25 min, (b) 8 h, (c) 16 h; slurrying conditions: 65°C and $L/S = 10/1$.

3. Results and discussion

3.1. XRD analysis

As seen in Fig. 1, the X-ray diffraction patterns of the sorbents prepared with various $Ca(OH)_2$/silica fume ratios show the existence of $Ca(OH)_2$, silica fume, and CSHs. The pattern of silica fume shows a mild hump with a peak at 2θ of about 23°, characterizing its amorphism. The peaks of calcium silicate hydrates (CSHs) are weak and belong to illcrystallized tobermorites ($2\theta = 29.0°$–$29.8°$, 32°, and 49.8°). Illcrystallized tobermorites include C–S–H(I), C–S–H(II), and tobermorite gel (Taylor, 1964). Under the present experimental conditions, they are mainly C–S–H(I), which is the same as the type of CSHs formed in the $Ca(OH)_2$/fly ash sorbents prepared by Ho and Shih (1992, 1993). As the ratio decreases, the characteristic peaks of $Ca(OH)_2$ become weaker and are not discernible when the ratio is smaller than 7/3, whereas the characteristic hump of silica fume becomes more marked. The characteristic peaks of CSHs are stronger for the sorbents with ratios of 7/3, 5/5, and 3/7, indicating that more CSHs had been formed in these sorbents than in the sorbents with 9/1 and 1/9 ratios.

In Fig. 2, no significant changes of the intensities of the characteristic peaks are observed for the sorbents prepared with slurrying times from 25 min to 16 h. This may indicate that the pozzolanic reaction between $Ca(OH)_2$ and silica fume in the slurry was very fast and had already reached the ultimate extent or drastically slowed down before 25 min, and thus there was no or too little increment of CSHs to be detected during the period from 25 min to 16 h. The pozzolanic reaction involving silica fume has been reported to be rapid by Grutzeck et al. (1983); the specific surface area of the silica fume and the slurrying temperature used in this study (220 m^2/g, 60°C) are much greater than theirs (20.2 m^2/g, 21–38°C), hence a very fast reaction can be expected for the present study.

One can note that in Fig. 1, the characteristic hump of silica fume is still present in the patterns of the sorbents with ratios of 9/1 and 7/3, but it is not so obvious in the patterns of the sorbents with a ratio of 7/3 shown in Fig. 2. This difference is thought to be caused by the variation of sampling. Nevertheless, the existence of silica fume in these two sorbents indicates that the CSHs tended to cohere with other particles, and some silica fume particles were covered by the CSHs and remained unreacted.

The calcium silicate hydrate C–S–H(I) is represented by the molecular formula $x\mathrm{CaO} \cdot \mathrm{SiO_2} \cdot y\mathrm{H_2O}$, where x is 0.8–1.5, and y is 0.5–2.5 (Taylor, 1964). According to the XRD results described above, the value of x was estimated to lie between 0.81 and 1.89 that are corresponding to $Ca(OH)_2$/silica fume ratios of 5/5 and 7/3, respectively. Weight measurements of the sorbents, however, showed that the weight of a dry sorbent was about equal to the weight of its starting $Ca(OH)_2$ and silica fume mixture. Thus the values of x and y for the CSHs formed in this study were about equal to 1.

3.2. SEM observation

Fig. 3(a) shows particles of the mixture of silica fume and $Ca(OH)_2$ before slurrying. The darker particles are silica fume, and the brighter ones are $Ca(OH)_2$. The particles of silica fume seen are agglomerates of very fine primary particles; according to the specification of the silica fume, the diameters of primary particles are in the range of 10–30 nm.

As shown in Fig. 3(b), the particles of the sorbent with a ratio of 9/1 are similar to those of the slurried $Ca(OH)_2$, but some large porous particles formed by CSHs are also present.

Figs. 3(c) and (d) are the SEM micrographs of the sorbent with a ratio of 7/3. Particles of this sorbent appear to be quite

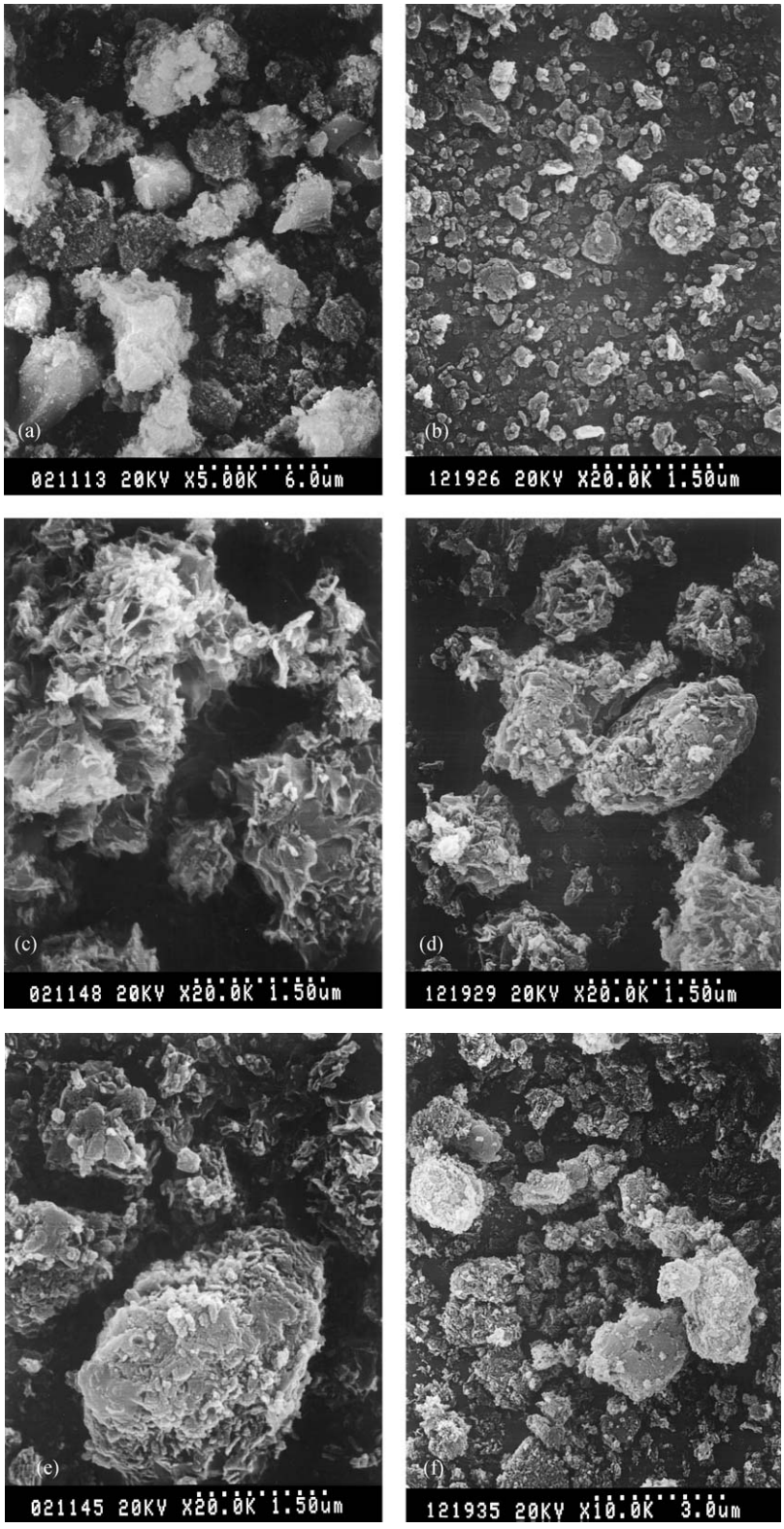

Fig. 3. SEM micrographs of $Ca(OH)_2$/silica fume sorbents. (a) Unslurried $Ca(OH)_2$/silica fume (wt. ratio 7/3) mixture. (b) $Ca(OH)_2$/silica fume (wt. ratio 9/1) sorbent; slurrying conditions: 65°C, 16 h, and $L/S = 10/1$. (c) and (d) $Ca(OH)_2$/silica fume (wt. ratio 7/3) sorbent; slurrying conditions: 65°C, 1 and 16 h, and $L/S = 10/1$. (e) $Ca(OH)_2$/silica fume (wt. ratio 5/5) sorbent; slurrying conditions: 65°C, 16 h, and $L/S = 10/1$. (f) $Ca(OH)_2$/silica fume (wt. ratio 3/7) sorbent; slurrying conditions: 65°C, 16 h, and $L/S = 10/1$.

Table 2
Structural properties and sulfation results for $Ca(OH)_2$/silica fume sorbents; slurrying conditions: 65°C and $L/S = 10/1$; sulfation conditions: 60°C, 70% RH, 1000 ppm SO_2, and 1 h

$Ca(OH)_2$/Silica fume weight ratio	Slurrying time (h)	Mean diameter (μm)	Surface area (m^2/g)	Utilization of Ca (mol SO_2/mol Ca)	SO_2 capture (kg SO_2/kg sorbent)
10/0	0	7.4	9.6	0.197	0.170
10/0	16	4.9	11.8	0.243	0.210
0/10	0	6.3	220.0	—	—
0/10	16	7.8	189.9	—	0.038
7/3	0.42	6.8	118.4	0.842	0.510
7/3	1	7.8	115.9	0.862	0.522
7/3	4	7.2	124.4	0.865	0.524
7/3	8	6.1	120.6	0.866	0.524
7/3	16	6.4	123.3	0.868	0.525
9/1	16	4.9	49.1	0.528	0.411
5/5	16	9.8	91.3	0.952	0.412
3/7	16	8.5	257.6	1.160	0.301
1/9	16	6.0	191.3	1.346	0.116

porous. Some particles are seen to be made up of thin foils of CSHs (Ho & Shih, 1992, 1993; Grutzeck et al., 1983) and have more open structure (Fig. 3(c)), while some particles are more compact and on their surfaces many small granular particles are attached (Fig. 3(d)). There was no significant difference in the morphologies of the sorbents prepared with a ratio of 7/3 and slurrying times of 0.42–16 h.

The particles of the sorbent with a ratio of 5/5, as shown in Fig. 3(e), are mainly the compact particles with many small granular particles attached on the surfaces; fewer particles with the open structure as that shown in Fig. 3(c) are observed, and the foils of CSHs seem to be thicker or become plates.

As shown in Fig. 3(f), some particles of the sorbent with a ratio of 3/7 are similar to those of the sorbent with a ratio of 5/5, but more highly porous particles of silica fume are present, and wispy foil-like substances are seen to reside in those particles.

The sorbent with a ratio of 1/9 and the slurried silica fume had the same particle appearance as that of the starting silica fume shown in Fig. 3(a).

3.3. Particle size distribution

The particle size distributions of the sorbents were measured and their volume mean diameters, being in the range of 4.9–9.8 μm, are summarized in Table 2. The mean diameter of the slurried $Ca(OH)_2$ sample, 4.9 μm, was smaller than that of the starting $Ca(OH)_2$, 7.4 μm, indicating that the dissolution and recrystallization of $Ca(OH)_2$ in the slurrying and drying processes, respectively, had produced finer $Ca(OH)_2$ particles (Ho & Shih, 1992). The mean diameter of the slurried silica fume sample, 7.8 μm, was close to that of the starting material, 6.3 μm; the particle sizes measured were those of the agglomerates of very fine primary particles.

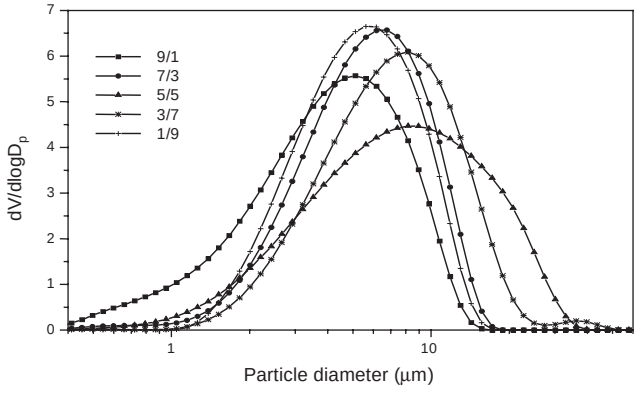

Fig. 4. Particle size distributions of $Ca(OH)_2$/silica fume sorbents prepared with various weight ratios; slurrying conditions: 65°C, 16 h, and $L/S = 10/1$.

The sorbents prepared with 25 min to 16 h slurrying times had about the same particle size distribution, but the sorbents prepared with various $Ca(OH)_2$/silica fume ratios had different size distributions. With the decrease of the ratio, the distribution curve shown in Fig. 4 shifts to the range of larger particle size until the ratio is 5/5, with which the sorbent has the largest volume mean diameter and the widest size distribution; the curve shifts to the range of smaller size thereafter. This trend of particle size change was confirmed by SEM observations and agreed with the CSHs amount in a sorbent estimated from XRD analyses. Thus, it can be concluded that the particle size distribution of a sorbent was related not only to the weight fractions and the particle sizes of $Ca(OH)_2$ and silica fume but also to the fraction

of CSHs, which can cause the coherence of particles in the sorbent.

3.4. Specific surface area

The specific surface areas of the sorbents are summarized in Table 2. Except the sorbent with a ratio of 5/5, all other $Ca(OH)_2$/silica fume sorbents have larger surface areas than those estimated for the starting mixtures, indicating the formation of new materials in the sorbents. The change of specific surface area with the ratio is not simple; there are two local maximum specific surface areas, 123.3 and 257.6 m^2/g, at ratios of 7/3 and 3/7, respectively. The influence of the $Ca(OH)_2$/silica fume weight ratio on the sorbent specific surface area can be explained by referring to the XRD analysis (Fig. 1) and SEM observation (Fig. 3). For the ratio of 9/1, the specific surface area of the sorbent was larger than that of $Ca(OH)_2$ alone because some part of $Ca(OH)_2$ had been converted to CSHs. For the ratio of 7/3, the amount of foils of CSHs formed in the sorbent increased, resulting in a further increase of the specific surface area; but for the ratio of 5/5, more compacted particles composed of plates and granular particles were formed, thus the specific surface area decreased. For the ratio of 3/7, with a great increase in the amount of very fine foils and particles in the sorbent, the specific surface area increased accordingly and was larger than that of the slurried silica fume. For the ratio of 1/9, the amount of CSHs formed in the sorbent was little, so the specific surface area of the sorbent was nearly equal to that of the slurried silica fume.

The effect of the slurrying time on the specific surface area was small, indicating that the amount of CSHs and the microstructure of the sorbent remained almost the same during the period of slurrying from 25 min to 16 h. XRD analyses (Fig. 2) and SEM observations confirmed this explanation.

3.5. Pore volume distribution

The nitrogen adsorption and desorption isotherms for the $Ca(OH)_2$/silica fume sorbents, not shown here, showed that all the sorbents exhibited a type IV isotherm and a type H3 hysteresis based upon the classification of IUPAC (1985). The type IV isotherm is characteristic of materials with porosity in the mesopore range and that typically exhibits a hysteresis loop, and the type H3 hysteresis is associated with slit-shaped pores or the space between platelike particles.

The pore volume distributions of the sorbents were obtained by applying the BJH method to the nitrogen desorption data for pores smaller than 300 nm. The results for $Ca(OH)_2$, silica fume, and the sorbent with a ratio of 7/3 are shown in Fig. 5. One can see that the pore volume distribution of the $Ca(OH)_2$/silica fume sorbent is broader than that of $Ca(OH)_2$ or silica fume alone, and the peak pore volumes of the three sorbents occur at about 22–32 nm pore diameter. Cumulative data showed that mesopores

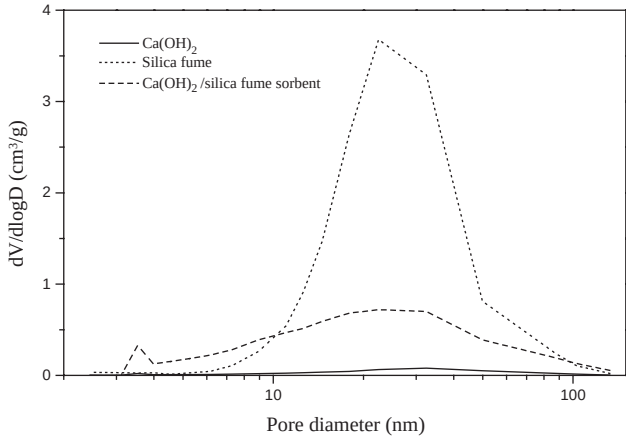

Fig. 5. Pore volume distributions of $Ca(OH)_2$, silica fume, and $Ca(OH)_2$/silica fume sorbent (wt. ratio 7/3); slurrying conditions: 65°C, 16 h, and $L/S = 10/1$.

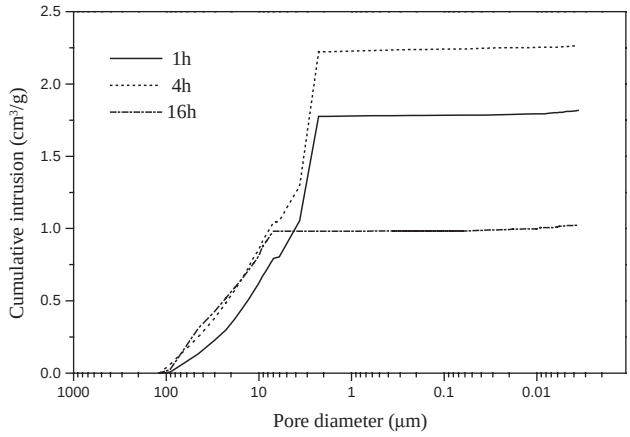

Fig. 6. Pore volume distributions of $Ca(OH)_2$/silica fume sorbents (wt. ratio 7/3) prepared with various slurrying times; slurrying conditions: 65°C and $L/S = 10/1$; measured by mercury intrusion method.

(2 nm $\leqslant$ pore dia. $\leqslant$ 50 nm) occupied the most portion of the total sorbent pore volume (pore dia. $\leqslant$ 300 nm), while the volume of micropores (pore dia. $\leqslant$ 2 nm) was very small. The specific total pore volume of silica fume, 1.85 cm^3/g, was about ten times that of $Ca(OH)_2$ and three times that of the $Ca(OH)_2$/silica fume sorbent.

The pore volume distributions of some sorbents with a ratio of 7/3 were also measured by mercury intrusion method; the results are shown in Fig. 6. The differences in the volumes of intrusion for pore sizes larger than 2 μm are due to the random arrangement of each sorbent in the sample cell. The pore volumes determined from the intrusion volumes for pores smaller than 1 μm can be seen to be very small. This is in contradiction to the results obtained by N_2 adsorption/desorption. The erroneous results of mercury intrusion measurements are probably due to the fact that the particles made up of silica fume and CSHs were compressible under high pressures.

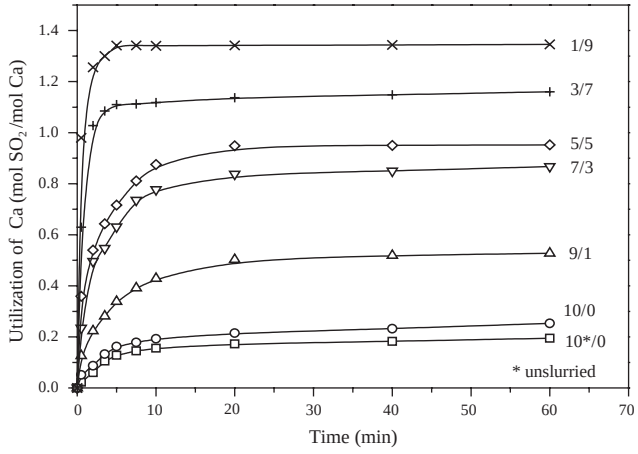

Fig. 7. Effect of $Ca(OH)_2$/silica fume weight ratio on the utilization of Ca for $Ca(OH)_2$/silica fume sorbents; slurrying conditions: 65°C, 16 h, and $L/S = 10/1$; sulfation conditions: 60°C, 70% RH, and 1000 ppm SO_2.

3.6. Reactivities of sorbents

The sorbents were subjected to sulfation tests at 60°C, 70% RH, and 1000 ppm SO_2 up to 1 h. The results for the sorbents with different $Ca(OH)_2$/silica fume ratios are shown in Fig. 7 in terms of the utilization of Ca versus reaction time. As seen from the figure, at the same reaction time, the utilization of Ca of sorbent increases remarkably with decreasing $Ca(OH)_2$/silica fume ratio. The utilization of Ca of sorbent levels off early before the reaction time reaches 60 min, thus the 1 h value represents the maximum utilization of Ca of each sorbent.

The 1 h results for all the sorbents tested are summarized in Table 2 in terms of the utilization of Ca and the SO_2 capture. The sorbents prepared with a ratio of 7/3 and different slurrying times from 0.42 to 16 h had about the same reactivity. This is because their compositions and physical properties were about the same. There was no data of the utilization of Ca for silica fume because it contained negligible amount of Ca. Although silica fume did not react with SO_2, it was able to adsorb SO_2 and had a SO_2 capture of 0.038 kg SO_2/kg of silica fume.

Fig. 8 shows the 1 h utilization of Ca as a function of the silica fume content in the starting solid mixture. The utilization of Ca increases considerably with increasing silica fume content. The values are higher than 1.0 for the sorbents prepared with silica fume contents of 70 and 90 wt%. The true utilizations of Ca in these two sorbents might have already reached 1.0, and the extra amounts of SO_2 captured are believed to be due to the adsorption of SO_2 by the sorbents because the specific surface areas of these two sorbents were very large. The extra amounts of SO_2 captured for these two sorbents were calculated to be 0.042 and 0.030 kg SO_2/kg sorbent, respectively, which are close to the SO_2 capture of silica fume.

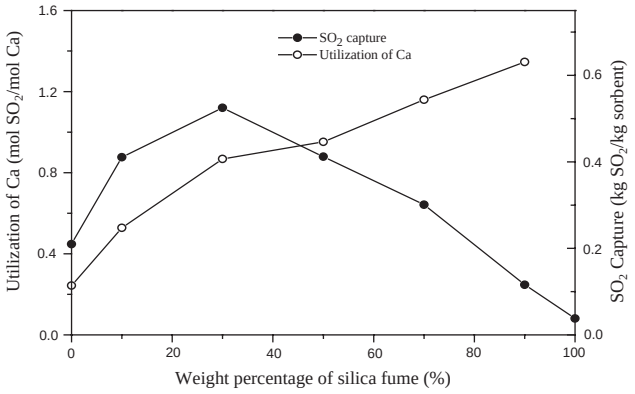

Fig. 8. Effect of the weight percentage of silica fume on the utilization of Ca and the SO_2 capture for $Ca(OH)_2$/silica fume sorbents; slurrying conditions: 65°C, 16 h, and $L/S = 10/1$; sulfation conditions: 60°C, 70% RH, 1000 ppm SO_2, and 1 h.

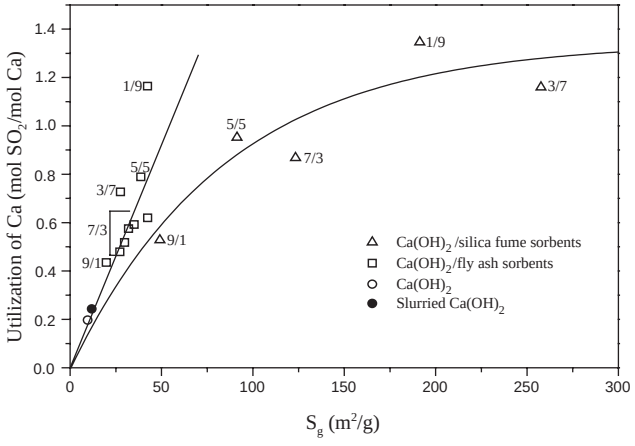

Fig. 9. Effect of specific surface area on the utilization of Ca for $Ca(OH)_2$/silica fume sorbents, $Ca(OH)_2$/fly ash sorbents, and $Ca(OH)_2$; slurrying conditions: 65°C, 16 h, and $L/S = 10/1$; sulfation conditions: 60°C, 70% RH, 1000 ppm SO_2, and 1 h.

The SO_2 capture as a function of the silica fume content is also shown in Fig. 8. The SO_2 capture increases as the silica fume content increases, reaching a maximum, 0.525 kg SO_2/kg sorbent, when the content is 30 wt%; a further increase of the content results in a gradual decrease in the SO_2 capture. As estimated from Fig. 8, the sorbents prepared with a $Ca(OH)_2$ content less than 100 wt% and greater than 21 wt% would have a SO_2 capture greater than that of $Ca(OH)_2$ alone. The difference in the trends of the utilization of Ca and the SO_2 capture can be explained by referring to Eq. (1). The value of M^{-1} in the equation decreases as the content of silica fume increases.

3.7. Effect of sorbent specific surface area

The effect of the specific surface area on the reactivity of sorbent was explored in Figs. 9 and 10.

As shown in Fig. 9, although the 1 h utilization of Ca did not increase monotonically with increasing specific surface

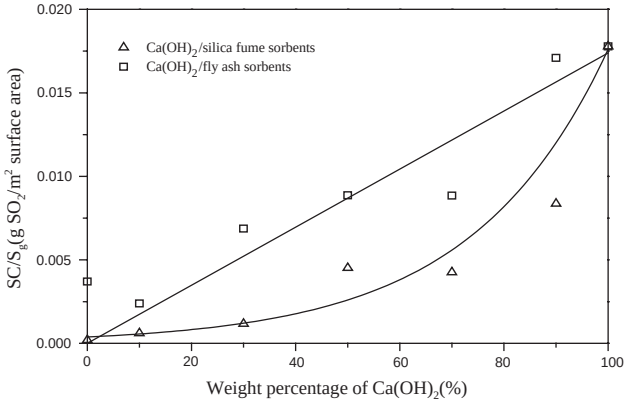

Fig. 10. Effect of the weight percentage of $Ca(OH)_2$ on the weight of SO_2 captured per unit surface area for $Ca(OH)_2$/silica fume and $Ca(OH)_2$/fly ash sorbents; slurrying conditions: 65°C, 16 h, and $L/S = 10/1$; sulfation conditions: 60°C, 70% RH, 1000 ppm SO_2, and 1 h.

area, the general trend of the data, represented by the fitting curve, indicates that it increases as the specific surface area increases, and exceeds 1.0 at about 120 m^2/g. The two sorbents with $Ca(OH)_2$ contents of 10 and 30 wt%, which had specific surface areas larger than 190 m^2/g, had utilizations of Ca greater than 1.0. As discussed before, the true utilizations of Ca in these two sorbents might have already reached 1.0, and the excess utilizations of Ca are thought to be contributed by SO_2 adsorption due to the large surface areas of these two sorbents. The SO_2 adsorption capacities based on unit weight or unit surface area for these two sorbents were estimated to be close to that for silica fume. From Table 2 and Fig. 10, one can see that the SO_2 capture capacity of silica fume was a lot smaller than those of sorbents with large $Ca(OH)_2$ contents. Therefore, the contribution of SO_2 adsorption to the utilization of Ca must be smaller for sorbents with smaller surface areas.

Fig. 10 shows that the amount of SO_2 captured (1 h) per unit surface area of sorbent, SC/S_g, increases with increasing $Ca(OH)_2$ content. But this trend deviates negatively from the linear relationship with the $Ca(OH)_2$ content. Furthermore, by looking into the values of SC/S_g and S_g of each sorbent, one can find that SC/S_g decreased with increasing S_g in general.

3.8. Comparison of reactivities of $Ca(OH)_2$/silica fume and $Ca(OH)_2$/fly ash sorbents

The variation trend of the 1 h utilization of Ca or SO_2 capture with the content of $Ca(OH)_2$ for the $Ca(OH)_2$/silica fume sorbents was similar to that for the $Ca(OH)_2$/fly ash sorbents prepared and sulfated under the same conditions of this study (Lin et al., 2002); both kinds of sorbents had the maximum SO_2 capture at a $Ca(OH)_2$ content of 70 wt%, but the maximum value for the latter sorbents, 0.375 kg SO_2/kg sorbent, was smaller. The utilizations of Ca for the $Ca(OH)_2$/fly ash sorbents are also plotted in Fig. 9 for comparison. At the same $Ca(OH)_2$ content, the utilization of Ca and the specific surface area of the $Ca(OH)_2$/fly ash sorbent are smaller, and there is roughly a linear relationship between the utilization of Ca and S_g; the slope of the straight fitting line is greater than that of the fitting curve for the $Ca(OH)_2$/silica fume sorbents. In other words, the utilization of Ca per unit specific surface area of sorbent, which has the physical meaning of weight of sorbent reacted per unit surface area, is almost constant for the $Ca(OH)_2$/fly ash sorbents, but that for the $Ca(OH)_2$/silica fume sorbents is smaller and decreases in general with increasing specific surface area.

The above comparison indicates that at the same $Ca(OH)_2$ content, the SO_2 capture capacity of the surface of the $Ca(OH)_2$/silica fume sorbent was lower than that of the $Ca(OH)_2$/fly ash sorbent. This is confirmed by comparing the SC/S_g data for both kinds of sorbents in Fig. 10. As discussed before, the surface area of a $Ca(OH)_2$/silica fume sorbent consisted of those of $Ca(OH)_2$, CSHs, and silica fume, and silica fume had large specific surface area, but the SO_2 capture capacity of the surface of silica fume was much less than that of $Ca(OH)_2$ or CSHs. Thus, the lower SO_2 capture capacity of the surface of the $Ca(OH)_2$/silica fume sorbent is due to the presence of the large surface area of silica fume in the sorbent. However, the specific surface areas of $Ca(OH)_2$ and CSHs in the $Ca(OH)_2$/silica fume sorbent might be greater than those in the $Ca(OH)_2$/fly ash sorbent, therefore the total utilization of Ca and SO_2 capture of the former sorbent were higher than those of the latter sorbent.

The above results indicate that silica fume, or other amorphous silicas with high surface areas, can be used to prepare sorbents with high reactivities toward SO_2.

4. Conclusions

$Ca(OH)_2$/silica fume sorbents have been prepared with different $Ca(OH)_2$/silica fume weight ratios and slurrying times at 65°C and a water/solid ratio of 10/1, and their reactivities toward SO_2 have been measured under the conditions of 60°C, 70% RH, and 1000 ppm SO_2.

The reaction between $Ca(OH)_2$ and silica fume to form CSHs(C–S–H(I)) in slurry was very fast and reached the ultimate extent within 25 min; more CSHs were formed for $Ca(OH)_2$/silica fume ratios of 3/7, 5/5, and 7/3 than for ratios of 1/9 and 9/1. The formation of CSHs resulted in sorbent particles with a highly porous structure that seemed compressible under high pressures. The sorbents were mesoporous and their specific surface areas and pore volumes were much larger than those of $Ca(OH)_2$ alone.

When the sorbents reacted with SO_2, the initial conversion rate and the 1 h utilization of Ca of sorbent increased with increasing silica fume content, mainly due to the increase in the specific surface area of sorbent with increasing silica fume content; the contribution of SO_2 adsorption was

appreciable for sorbents with high silica fume contents. The 1 h SO_2 capture of sorbent had a maximum (0.525 kg SO_2/kg sorbent) at 30 wt% silica fume. Sorbents with $Ca(OH)_2$ contents less than 100 wt% and greater than 21 wt% would have a SO_2 capture greater than that of $Ca(OH)_2$ alone. Both the 1 h utilization of Ca and SO_2 capture per unit specific surface area of sorbent decreased in general with increasing specific surface area. At the same $Ca(OH)_2$ content, the 1 h utilization of Ca or SO_2 capture of the $Ca(OH)_2$/silica fume sorbent was greater than that of the $Ca(OH)_2$/fly ash sorbent; however, the amount of SO_2 captured per unit surface area of the former sorbent was smaller than that of the latter sorbent due to the presence of the large surface area of silica fume in the former sorbent.

Silica fume, or other amorphous silicas with high surface areas, can be used with $Ca(OH)_2$to prepare sorbents with high reactivities toward SO_2.

Notation

M	initial sorbent weight per mole of Ca, g sorbent/mol Ca
M_{SO_2}	molecular weight of SO_2, g/mol
RH	relative humidity, %
SC	SO_2 capture, kg SO_2/kg sorbent
S_g	initial specific surface area, m^2/g

Acknowledgements

This research was supported by the National Science Council of Republic of China (Taiwan).

References

Al-Shawabkeh, A., Matsuda, H., & Hasatani, M. (1995). Utilization of highly improved fly ash for SO_2 captures. *Journal of Chemical Engineering of Japan*, *28*, 53–58.

Chiang, S. T. (1994). *The kinetic study of the reaction of $Ca(OH)_2/SiO_2$ sorbent with SO_2*. MS. Engineering thesis, Department of Chemical Engineering, National Taiwan University, Taipei, Taiwan.

Chiu, C. S. (1989). *The reactivity of $Ca(OH)_2/SiO_2$ sorbent with SO_2*. MS. Engineering thesis, Department of Chemical Engineering, National Taiwan University, Taipei, Taiwan.

Diffenbach, P., Hilterman, M., Frommell, E., Boother, H., & Hedges, S. (1991). Characterization of calcium oxide-fly ash sorbent for SO_2 removal. *Thermochimica Acta*, *189*, 1–24.

Fernández, J., Renedo, M. J., Garea, A., Viguri, J. R., & Irabien, J. A. (1997). Preparation and characterization of fly ssh/hydrated lime sorbents for SO_2 removal. *Powder Technology*, *94*, 133–139.

Garea, A., Fernández, I., Viguri, J. R., Ortiz, M. I., Renedo, M. J., & Irabien, J. A. (1997a). Fly ash/calcium hydroxide mixtures for SO_2 removal: Structural properties and maximum yield. *Chemical Engineering Journal*, *66*, 171–179.

Garea, A., Viguri, J. R., & Irabien, J. A. (1997b). Kinetics of the flue gas desulfurization at low temperature: Fly ash/calcium (3/1) sorbent behavior. *Chemical Engineering Science*, *52*, 715–732.

Grutzeck, M. W., Atkmson, S., & Roy, D. M. (1983). Mechanism of hydration of condensed silica fume in calcium hydroxide solution. In V. M. Malhotra (Ed.), *Fly ash, silica fume, slag & other minerals. By-products in concrete*, Vol. II (pp. 643–664). Publication SP-79, American Concrete Institute, Detroit, Michigan.

Ho, C. S., & Shih, S. M. (1992). $Ca(OH)_2$/fly ash sorbents for SO_2 removal. *Industrial and Engineering Chemical Research*, *31*, 1130–1135.

Ho, C. S., & Shih, S. M. (1993). Characteristic and SO_2 capture capacities of sorbents prepared from products of spray-drying flue gas desulfurization. *Canadian Journal of Chemical Engineering*, *71*, 934–939.

Ishizuka, T., Tsuchiai, H., Murayama, T., Tanaka, T., & Hattori, H. (2000). Preparation of active absorbent for dry-type flue gas desulfurization from calcium oxide, coal fly ash, and gypsum. *Industrial and Engineering Chemical Research*, *39*, 1390–1396.

IUPAC (1985). Reporting physisorption data for gas/solid systems with special reference to the determination of surface area and porosity. *Pure and Applied Chemistry*, 57, 603–619.

Jozewicz, W., Chang, J. C. S., Sedman, C. B., & Brna, T. G. (1988a). Silica-enhanced sorbents for dry injection removal of SO_2 from flue gas. *Journal of Air Pollution Control Association*, *38*, 1027–1034.

Jozewicz, W., Jorgensen, C., Chang, J. C. S., Sedman, C. B., & Brna, T. G. (1988b). Development and pilot plant evaluation of silica-enhanced lime sorbents for dry flue gas desulfurization. *Journal of Air Pollution Control Association*, *38*, 796–805.

Jozewicz, W., & Rochelle, G. T. (1986). Fly ash recycle in dry scrubbing. *Environmental Progress*, *5*, 219–224.

Jung, G. H., Kim, H., & Kim, S. G. (2000a). Preparation and characterization of lime-silica solids. *Industrial and Engineering Chemical Research*, *39*, 1264–1270.

Jung, G. H., Kim, H., & Kim, S. G. (2000b). Utilization of lime-silica solids for flue gas desulfurization. *Industrial and Engineering Chemical Research*, *39*, 5012–5016.

Kind, K. K. (1994). *Hydrothermal preparation of high surface area calcium silicate from lime and fly ash in a flow reactor*. Ph.D. dissertation, Department of Chemical Engineering, University of Texas at Austin.

Kind, K. K., & Rochelle, G. T. (1994). Preparation of calcium silicate reagent from fly ash and lime in a flow reactor. *Journal of Air and Waste Management Association*, *44*, 869–876.

Kind, K. K., Wasserman, P. D., & Rochelle, G. T. (1994). Effects of salts on preparation and use of calcium silicates for flue gas desulfurization. *Environmental Science and Technology*, *28*, 277–283.

Lin, R. B. (1998). *Preparation and characterization of $Ca(OH)_2$/silica fume and $Ca(OH)_2$/fly ash sorbents for desulfurization*. MS. Engineering thesis, Department of Chemical Engineering, National Taiwan University, Taipei, Taiwan.

Lin, R. B., Shih, S. M., & Liu, C. F. (2002). Reactivities of *$Ca(OH)_2$/fly* ash sorbents for flue gas desulfurization. *Proceedings of the 20th ROC symposium on catalysis and reaction engineering*, Tainan, Taiwan (pp. 294–302).

Liu, C. F. (1999). *Kinetics of the reactions of $Ca(OH)_2$/silica fume and $Ca(OH)_2$/fly ash sorbents with SO_2*. MS. Engineering thesis, Department of Chemical Engineering, National Taiwan University, Taipei, Taiwan.

Liu, C. F., Shih, S. M., & Lin, R. B. (2002). Kinetics of the reactions of $Ca(OH)_2$/fly ash sorbents with SO_2 at low temperatures. *Chemical Engineering Science*, *57*, 93–104.

Martinez, J. C., Izquierdo, J. F., Cunill, F., Tejero, J., & Querol, J. (1991). Reactivation of fly ash and $Ca(OH)_2$ mixtures for SO_2 removal of flue gas. *Industrial and Engineering Chemical Research*, *30*, 2143–2147.

Miller, M. J. (1986). Retrofit SO_2 and NO_x control technologies for coal-fired power plants. *Environmental Progress*, *3*, 171–177.

Peterson, J. R. (1990). *Hydrothermal reaction of lime with fly ash to produce calcium silicates for dry flue gas desulfurization*. Ph.D. dissertation, Department of Chemical Engineering, University of Texas at Austin.

Peterson, J. R., & Rochelle, G. T. (1988). Aqueous reaction of fly ash and $Ca(OH)_2$ to produce calcium silicate absorbent for flue gas desulfurization. *Environmental Science and Technology*, *22*, 1299–1304.

Peterson, J. R., & Rochelle, G. T. (1990). Lime/fly ash materials for flue gas desulfurization effects of aluminum and recycle materials. *Proceedings of 1990 SO_2 control symposium*, New Orleans, LA (pp. P3–P24).

Renedo, M. J., Fernández, J., Garea, A., Ayerbe, A., & Irabien, J. A. (1999). Microstructural changes in the desulfurization reaction at low temperature. *Industrial and Engineering Chemical Research*, *38*, 1384–1390.

Sanders, J. R., Keener, T. C., & Wang, J. (1995). Heated fly ash/hydrated lime slurries for SO_2 removal in spray dryer absorbers. *Industrial and Engineering Chemical Research*, *34*, 302–307.

Srivastava, R. K., & Jozewicz, W. (2001). Flue gas desulfurization: The state of the art. *Journal of Air and Waste Management Association*, *51*, 1676–1688.

Taylor, H. F. W. (1964). *The chemistry of cement*. London: Academic Press.

Tsuchiai, H., Ishizuka, T., Ueno, T., Hattori, H., & Kita, H. (1995). Highly active absorbent for SO_2 removal prepared from coal fly ash. *Industrial and Engineering Chemical Research*, *34*, 1404–1411.